ANALYTICAL EXPRESSIONS FOR FRESNEL VOLUMES AND INTERFACE FRESNEL ZONES OF SEISMIC BODY WAVES. PART 2: TRANSMITTED AND CONVERTED WAVES. HEAD WAVES.

MICHAL KVASNIČKA, VLASTISLAV ČERVENÝ

*Department of Geophysics, Charles University, Prague**

Summary: *Fresnel volumes and interface Fresnel zones of transmitted and head waves are studied. The relation derived for transmitted waves may also be used for converted reflected waves. Considerable attention is devoted to the penetration of Fresnel volumes across structural interfaces, particularly for head waves.*

Keywords: Fresnel volumes, interface Fresnel zones, seismic body waves, seismic ray methods, first arrival travel times

1. INTRODUCTION

Whereas Part 1 of this paper (*Kvasnička and Červený, 1996*) was devoted to the Fresnel volumes and Fresnel zones of direct and reflected unconverted waves, this part discusses mainly the Fresnel volumes and Fresnel zones of transmitted and head waves generated at a plane interface between two homogeneous half-spaces.

For a detailed explanation of the concept of Fresnel volumes and Fresnel zones, for relevant definitions and various methods of computation see Part 1. We assume that the reader is familiar with Part 1 and shall try to avoid any repetition. We shall also give only a few references; for a very detailed list of references see Part 1. All figures of the Fresnel volumes and Fresnel zones presented in this paper have been computed by the method of network ray tracing, see *Kvasnička and Červený (1994)*.

2. FRESNEL VOLUMES AND FRESNEL ZONES OF HEAD WAVES

We shall consider a monochromatic head wave propagating along a plane interface Σ between two homogeneous media. We denote the velocity in the upper medium v_1 and in the bottom medium v_2, and assume that $v_2 > v_1$. Both source S and receiver R are situated in the upper medium, at the same distance h from interface Σ. The distance between S and R is denoted r.

If the distance r between the source and receiver is larger than the so-called critical distance r^*, the first arriving wave at the receiver is the *head wave*. The critical distance r^* is given by the relation

$$r^* = \frac{2hn}{\left(1-n^2\right)^{1/2}} \quad , \tag{1}$$

* Address: Ke Karlovu 3, 121 16 Praha 2, Czech Republic
(Fax: +42-2-21911292; e-mail: qasnicka@seis.karlov.mff.cuni.cz)

Studia geoph. et geod. 40 (1996), 381–397

where n is the refraction index, $n = v_1/v_2$. The ray of the head wave is composed of three elements, see Fig. 1b: *SA*, *AB*, and *BR*. The middle element *AB* is situated in the second medium, just below interface Σ, and is parallel to the interface. Thus, the ray parameter p^* of the head wave equals $p^* = \sin i^*/v_1 = 1/v_2$, as the angle of transmission equals ½ π. Angle $i^* = \sin^{-1}(v_1/v_2)$ is called the critical angle. We denote the length of ray element *AB*, parallel to Σ, by *L*,

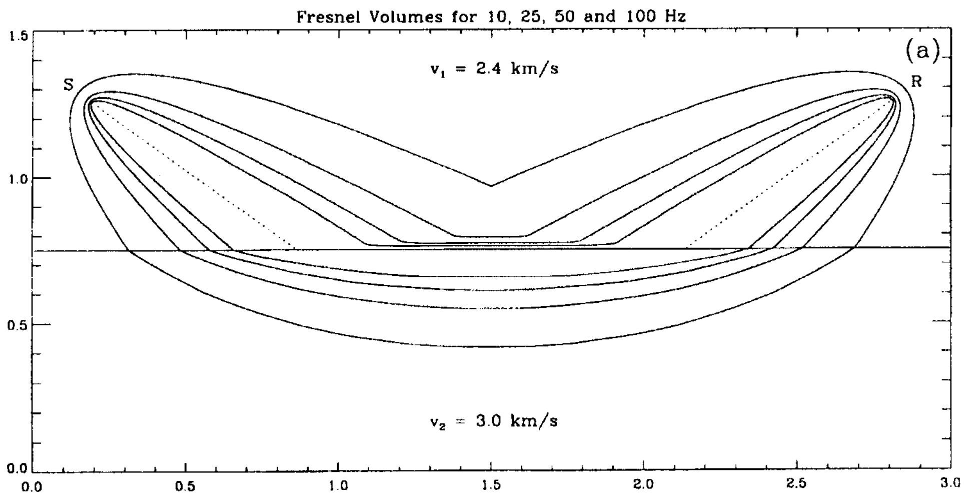

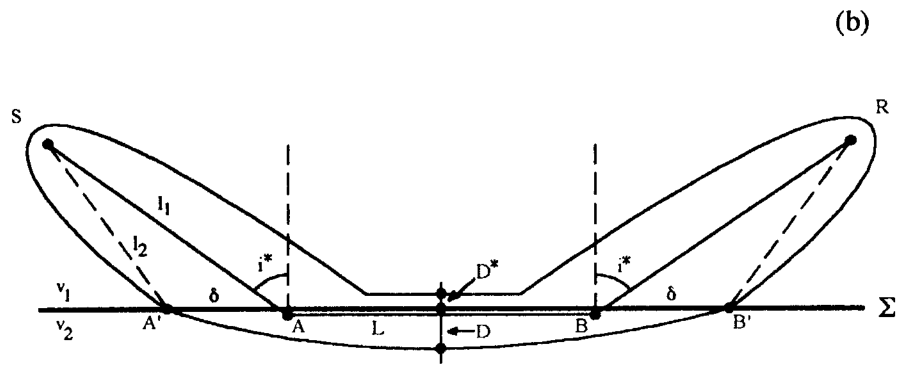

Fig. 1. (a) Boundaries of the Fresnel volumes of head waves for four frequencies f = 10, 25, 50 and 100 Hz. The distances of source *S* and receiver *R* from interface Σ are 0·5 km. The distance between source *S* and receiver *R* is 2·6 km. The velocity in the upper medium is 2.4 km/s, and in the lower medium 3 km/s. The Fresnel volume of the head wave penetrates into the upper velocity medium (containing *S* and *R*) also along the segment of the ray parallel to the interface. Penetration distance D^* is proportional to f^{-1}. (b) The boundary of the Fresnel volume of a head wave for frequency f = 25 Hz. Various notations.

$$L = r - r^* = r - \frac{2hn}{\left(1-n^2\right)^{1/2}} \quad . \tag{2}$$

Note that the Fresnel volumes and Fresnel zones of head waves cannot be calculated by Fresnel volume ray tracing, see *Červený and Soares (1992)*. The reason is that the head wave is not a zero-order wave in terms of the ray series solution.

2.1 The interface Fresnel zone of head waves

The Fresnel volumes and interface Fresnel zones of head waves have shapes considerably different from those of reflected waves, see Fig. 1a. The Fresnel volumes are not ellipsoidal and the interface Fresnel zones are not elliptical. A typical property of the interface Fresnel zone of a head wave is its large horizontal extent. We shall again speak of *in-plane and transverse semi-axes of the interface Fresnel zone* and denote them $r^{\parallel}$ and $r^{\perp}$. By $r^{\parallel}$ we shall understand one half of the maximum horizontal extent of the interface Fresnel zone. We define $r^{\perp}$ similarly.

The *in-plane semi-axis* $r^{\parallel}$ of the interface Fresnel zone of the head wave is given by the relation, see Fig. 1b,

$$r^{\parallel} = \frac{1}{2}L + \delta \quad . \tag{3}$$

Here δ is the length of interface element $\overline{A'A}$, and, due to the symmetry, also the length of $\overline{B'B}$. Quantity δ can be determined from the relation

$$\frac{\ell_2}{v_1} + \frac{\delta}{v_2} - \frac{\ell_1}{v_1} = \frac{1}{2}T \quad , \tag{4}$$

where

$$\ell_1 = \frac{h}{\cos i^*} \quad , \qquad \ell_2 = \left(\ell_1^2 + \delta^2 - 2\ell_1\delta\sin i^*\right)^{1/2} \quad . \tag{5}$$

This yields the quadratic equation for δ:

$$\left(1-n^2\right)\delta^2 + nv_1T\delta - \ell_1 Tv_1\left(1 + \frac{\frac{1}{4}v_1T}{\ell_1}\right) = 0 \quad .$$

The solution for positive δ is as follows:

$$\delta = \sqrt{\frac{\lambda_1\ell_1}{1-n^2}}\left(\sqrt{1 + \frac{1}{4}\frac{\lambda_1}{\ell_1\left(1-n^2\right)}} - \frac{1}{2}\sqrt{\frac{\lambda_1}{\ell_1}}\frac{n}{\sqrt{1-n^2}}\right) \quad , \tag{6}$$

where $\lambda_1 = v_1T = v_1/f$ is the wavelength in the first medium. Equation (6) for δ is exact. In the high-frequency approximation, (6) may be simplified:

$$\delta \approx \sqrt{\frac{\lambda_1 \ell_1}{1-n^2}} \left(1 - \frac{1}{2} \sqrt{\frac{\lambda_1}{\ell_1}} \frac{n}{\sqrt{1-n^2}} \right) \approx \sqrt{\frac{\lambda_1 \ell_1}{1-n^2}} \quad . \tag{7}$$

The first expression in (7) is valid up to terms with f^{-1}, but the second only up to terms with $f^{-1/2}$. We remind the reader that $n = v_1/v_2$. Using (3) and (6), we obtain the *final exact equation for the in-plane semi-axis of the interface Fresnel volume* $r^{\|}$ of the head waves,

$$r^{\|} = \frac{1}{2} L + \sqrt{\frac{\lambda_1 \ell_1}{1-n^2}} \left(\sqrt{1 + \frac{1}{4} \frac{\lambda_1}{\ell_1 (1-n^2)}} - \frac{1}{2} \sqrt{\frac{\lambda_1}{\ell_1}} \frac{n}{\sqrt{1-n^2}} \right) \quad . \tag{8}$$

The transverse semi-axis $r^{\perp}$ of the interface Fresnel zone of the head wave can be evaluated from the relation

$$\frac{2}{v_2} \left[\left(\left(\frac{r^*}{2} + \frac{L}{2} \right)^2 + r^{\perp 2} \right)^{1/2} - \left(\frac{r^*}{2} + \frac{L}{2} \right) \right] = \frac{1}{2} T \quad .$$

Here we have taken into account the assumption that both the source and receiver are situated at the same distance h from the interface. This can be expressed as follows:

$$\frac{r^{\perp 2}}{\left(\frac{r^2}{4} + r^{\perp 2} \right)^{1/2} + \frac{r}{2}} = \frac{v_2 T}{4} \quad . \tag{9}$$

Equation (9) is still exact. Assuming δ to be small, and taking into account that $r^* + L = r$, we obtain approximately

$$r^{\perp} \approx \frac{1}{2} \sqrt{\lambda_2 r} \quad , \tag{10}$$

where $\lambda_2 = v_2 T = v_2/f$ is the wavelength in the second medium. It is not surprising that (10) is the same as the HF equation for semi-axis b of the Fresnel volume of the direct wave in a homogeneous medium, see (7) for b in *Kvasnička and Červený (1996)*.

2.2 Penetration distances

We shall now seek approximate relations for penetration distances D and D^* below and above interfaxe Σ, see fig. 1b.

As in the case of reflected waves, we denote D the penetration distance of the Fresnel volume of a head wave below interface Σ (into the higher-velocity medium). In fact, we can again use the exact equation (36), derived in Section 3.2 of *Kvasnička and Červený (1996)*. We insert $p = 1/v_2$, as we are considering head waves. Equation (36) with equation $r = f_4(p')$ then yields the exact value of D.

Equation (36) with $r = f_4(p')$ can also be used to determine D approximately. For small D/L, p' is very close to $p = 1/v_2$, and the square root $\left(1 - v_2^2 p'^2\right)^{1/2}$ is very small. We can determine it from the equation $r = f_4(p')$:

$$\left(1 - v_2^2 p'^2\right)^{1/2} \approx 2\frac{D}{L} \quad . \tag{11}$$

Eq. (36) then reads

$$L(p' - p) + 4\frac{D^2}{v_2 L} \approx \frac{1}{2}T \quad . \tag{12}$$

Using (11), we can also calculate $p' - p \approx -2D^2/\left(v_2 L^2\right)$. Inserting it into (12) finally yields

$$D \approx \frac{1}{2}\sqrt{v_2 T L} \quad . \tag{13}$$

This is the final approximate expression for the penetration distance D of the Fresnel volume of the head wave below Σ.

The *penetration distance* D^* of the Fresnel volume of the head wave above the interface (from the higher-velocity medium into the lower-velocity medium) will be estimated only approximately here, see Fig. 2. We assume that L is large and consider only such a vicinity of the interface in the upper medium which does not belong to the descending (incident) or ascending (reflected) branches of the Fresnel volume. We shall consider a virtual point F above interface Σ and estimate its distance D^* from Σ. The requirement is that the time difference between trajectories a and b in Fig. 2 is ½T. From simple geometrical considerations, we obtain, see Fig. 2,

$$2D^*\left(\frac{1}{v_1 \cos i^*} - \frac{\tan i^*}{v_2}\right) = \frac{1}{2}T \quad , \tag{14}$$

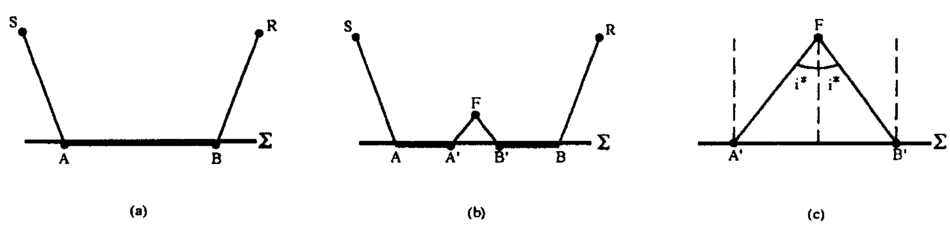

Fig. 2. Schematic diagrams for the computations of the penetration distance D^* of the head wave into the lower velocity upper medium. Part (a): Standard ray of the head wave. Part (b): Virtual point F is situated in the upper medium. Part (c): Enlargement of part (b) in the vicinity of virtual point F.

where $\sin i^* = n = v_1/v_2$. This immediately yields

$$D^* \approx \frac{1}{4} v_1 T\left(1-n^2\right)^{-1/2} \quad . \tag{15}$$

2.3 Numerical analysis

As we can see from Figs. 1 and 3, the interface Fresnel zones of head waves are considerably larger than the interface Fresnel zones of reflected waves. The in-plane semi-axis $r^{\parallel}$ of the interface Fresnel zone is always larger than $\frac{1}{2}L$, see Eqs. (3) and (8). For smaller h, $r^{\parallel}$ may even be close to $\frac{1}{2}r$, where r is the offset.

Let us discuss the numerical values of $r^{\parallel}$ using the example presented in Fig. 1a, computed by network ray tracing. In this case, $\frac{1}{2}L = 0{\cdot}63$ km and $\frac{1}{2}r = 1{\cdot}3$ km. The actual values of $r^{\parallel}$ are 1·18 km (for $f = 10$ Hz), 1·01 km (for $f = 25$ Hz), 0·91 km (for $f = 50$ Hz) and 0·84 km (for $f = 100$ Hz). These are in excellent agreement with the values of $r^{\parallel}$ measured in Fig. 1a. This is not surprising, as Eqs. (6) and (8) are exact. If, however, we take any of the approximate equations for δ given by (7) instead of that given by (6), the accuracy of δ and $r^{\parallel}$ will be lower. The error will increase with decreasing frequency f. For example, the error of the expression $\delta = \sqrt{\lambda_1 \ell_1 / \left(1-n^2\right)}$ for $f = 10$ Hz is close to 30% and the consequent error in $r^{\parallel}$ is close to 16%.

The expressions (13) for penetration distance D and (15) for D^* have been derived only approximately. Nevertheless, they provide very good agreement with the relevant quantities measured in Figs. 1a and 3.

In the derivation of all the equations of this section, we have assumed that distances of the source and receiver from the interface are the same, $h_S = h_R = h$. In Fig. 3, three examples of four correspond to $h_S \neq h_R$. Equation (15) for penetration distance D^* into the upper medium does not depend on h_S and h_R, if L is sufficiently large. That D^* is independent of h_S and h_R can be easily seen in Fig. 3. Equation (13) for the penetration distance D into the lower medium depends on h_S and h_R due to $L = r - \left(h_S + h_R\right) n / \sqrt{1-n^2}$. Thus, L increases with decreasing h_R. Consequently, D increases with decreasing h_R, see (13). This increase of D with decreasing h_R can be observed in Fig. 3, but it is not very distinct. Again, the values of D calculated using (13) agree very well with those measured from Fig. 3.

Similarly, Eq. (3) for $r^{\parallel}$ can be modified for $h_S \neq h_R$ by putting $r^{\parallel} = L/2 + (\delta_S + \delta_R)/2$, where δ_S and δ_R are given by (6) and are calculated independently at S and R. Only ℓ_1 will be different in both these expressions.

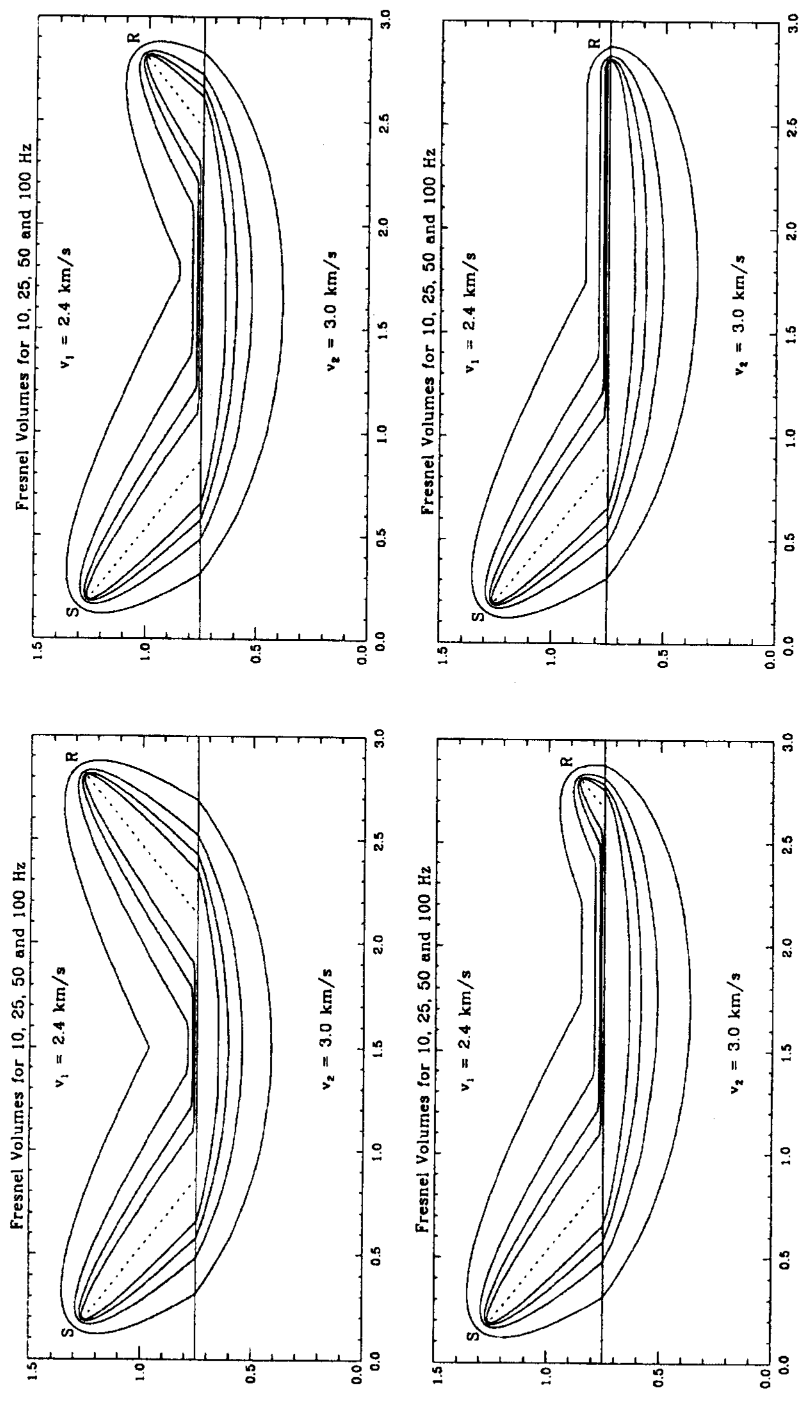

Fig. 3. Boundaries of the Fresnel volumes of head waves for four different distances of receiver *R* from interface Σ: $h_R = 0{\cdot}5$, $0{\cdot}25$, $0{\cdot}1$ and 0 km. Offset *r* is the same in all frames, $r = 2{\cdot}6$ km. All other parameters are the same as in Fig. 1.

3. FRESNEL VOLUMES AND INTERFACE FRESNEL ZONES OF TRANSMITTED WAVES

In this section, we shall discuss the Fresnel volumes and interface Fresnel zones of *transmitted waves* at a plane interface Σ between two homogeneous media. The results will also apply to *converted waves* at a plane interface, both reflected and transmitted, provided the velocities are specified properly. See also *Eaton et al. (1991)*, *Hubral et al. (1993)*.

We assume that the source is situated in the first medium at point S, and the receiver in the second medium at point R. The velocity in the first medium, v_1, will also be alternatively denoted v_S, and the velocity in the second medium, v_2, v_R. Thus, refraction index n is given by relation $n = v_1/v_2 = v_S/v_R$. We further denote the point of incidence at Σ by Q, see Fig. 4. Trajectory SQR constitutes the ray of the transmitted wave, and Snell's law is satisfied at Q, $p = \sin i_S/v_S = \sin i_R/v_R$. We denote the length of elements $\overline{SQ}$ and $\overline{QR}$ by ℓ_S and ℓ_R, so that

$$\ell_S = \frac{h_S}{\cos i_S} \quad , \qquad \ell_R = \frac{h_R}{\cos i_R} \quad . \tag{16}$$

Here h_S and h_R are the distances of source S and receiver R from interface Σ, i_S is the angle of incidence and i_R the angle of transmission.

3.1 Interface Fresnel zones of transmitted waves

We now choose an arbitrary (virtual) point F on interface Σ and denote the distance of source S and receiver R from F by $\ell'_S = \overline{SF}$ and $\ell'_R = \overline{FR}$.

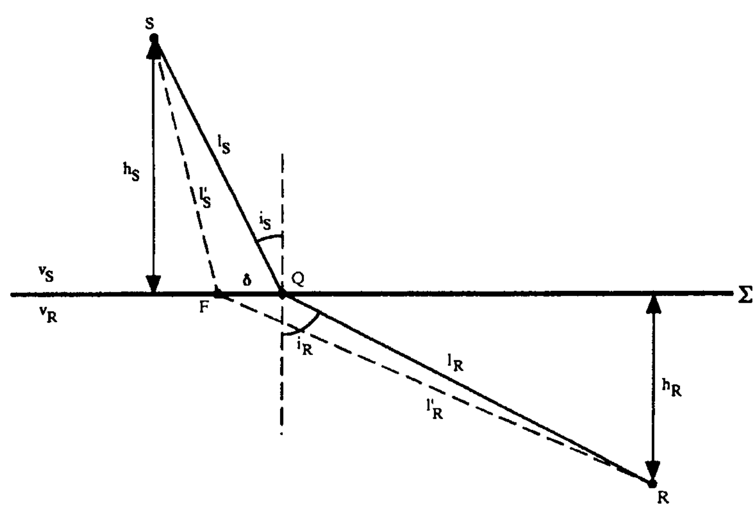

Fig. 4. Schematic diagram for the computation of the position of virtual point F on interface Σ for the transmitted wave, $\delta = \overline{FQ}$.

Note that elements ℓ'_S, ℓ'_R do not constitute a ray and that Snell's law is not satisfied at F.

We wish to determine the position of point F on Σ so that the travel time along SFR differs by ½T from the travel time along SQR. The basic equation for determining the position of point F thus reads

$$\frac{\ell'_R}{v_R}+\frac{\ell'_S}{v_S}-\frac{\ell_R}{v_R}-\frac{\ell_S}{v_S}=\frac{1}{2}T \quad . \tag{17}$$

We denote distance $\overline{QF}$ by δ, and express ℓ'_R, ℓ'_S in terms of ℓ_R, ℓ_S, δ and $p = \sin i_R/v_R = \sin i_S/v_S$:

$$\ell'_S=\left(\ell_S^2+\delta^2\mp 2\ell_S\delta\sin i_S\right)^{1/2}=\left(\ell_S^2+\delta^2\mp 2\ell_S v_S p\delta\right)^{1/2} \quad , \tag{18a}$$

$$\ell'_R=\left(\ell_R^2+\delta^2\pm 2\ell_R\delta\sin i_R\right)^{1/2}=\left(\ell_R^2+\delta^2\pm 2\ell_R v_R p\delta\right)^{1/2} \quad . \tag{18b}$$

Here the upper signs correspond to the points F situated on the left-hand side of Q, and the lower signs to the points F situated on the right-hand side of Q.

The ray parameter p in (18) can be determined from the relation for the horizontal range r between S and R,

$$r=p\left(\frac{h_S v_S}{\sqrt{1-v_S^2p^2}}+\frac{h_R v_R}{\sqrt{1-v_R^2p^2}}\right) \quad . \tag{19}$$

Equation (17) with ℓ'_S and ℓ'_R given by (18) can be used to determine *exactly* quantity δ in terms of h_S, h_R, v_S, v_R and ray parameter p. If we use the additional equation (19), δ can be determined in terms of h_S, h_R, v_S, v_R and horizontal range r. The latter case is, of course, more important in practical applications, but numerically more involved, as it requires the solution of (19) for p.

Now we seek an approximate solution of (17). By expanding ℓ'_S in terms of δ/ℓ_S and ℓ'_R in terms of δ/ℓ_R, up to second-order terms, Eq. (17) will yield

$$\frac{\delta^2}{2}\left(\left(\frac{1}{v_S\ell_S}+\frac{1}{v_R\ell_R}\right)-p^2\left(\frac{v_R}{\ell_R}+\frac{v_S}{\ell_S}\right)\right)\approx\frac{1}{2}T \quad . \tag{20}$$

Hence,

$$\delta\approx\sqrt{T}\left(\left(\frac{1}{v_S\ell_S}+\frac{1}{v_R\ell_R}\right)-p^2\left(\frac{v_R}{\ell_R}+\frac{v_S}{\ell_S}\right)\right)^{-1/2} \quad . \tag{21}$$

Alternatively,

$$\delta\approx\sqrt{T}\left(\frac{\cos^2 i_S}{\ell_S v_S}+\frac{\cos^2 i_R}{\ell_R v_R}\right)^{-1/2}\approx\sqrt{T}\left(\frac{\cos^3 i_S}{h_S v_S}+\frac{\cos^3 i_R}{h_R v_R}\right)^{-1/2} \quad . \tag{22}$$

3.2 The interface Fresnel zone of transmitted waves for modest angles of incidence

Equations (21) and (22) are very convenient for computing the dimensions of the interface Fresnel zone of transmitted waves for small angles of incidence. A typical shape of the Fresnel volume of a transmitted wave for such a situation is shown in Fig. 5.

The same expression for δ are obtained for the virtual points F situated on both sides of Q. Consequently, the *in-plane radius* $r^{\|}$ *of the interface Fresnel zone* of the transmitted wave is given by the relation

$$r^{\|} = \delta = \sqrt{T}\left(\frac{\cos^2 i_S}{v_S \ell_S} + \frac{\cos^2 i_R}{v_R \ell_R}\right)^{-1/2} \quad , \tag{23}$$

or by an alternative relation for δ in (21) and (22).

We shall now compute the *transverse semi-axis* $r^{\|}$ of the interface Fresnel zone of the transmitted wave. It ca again be calculated from (17), if we insert

$$\ell'_S = \left(\ell_S^2 + r^{\perp 2}\right)^{1/2} \quad , \qquad \ell'_R = \left(\ell_R^2 + r^{\perp 2}\right)^{1/2} \quad . \tag{24}$$

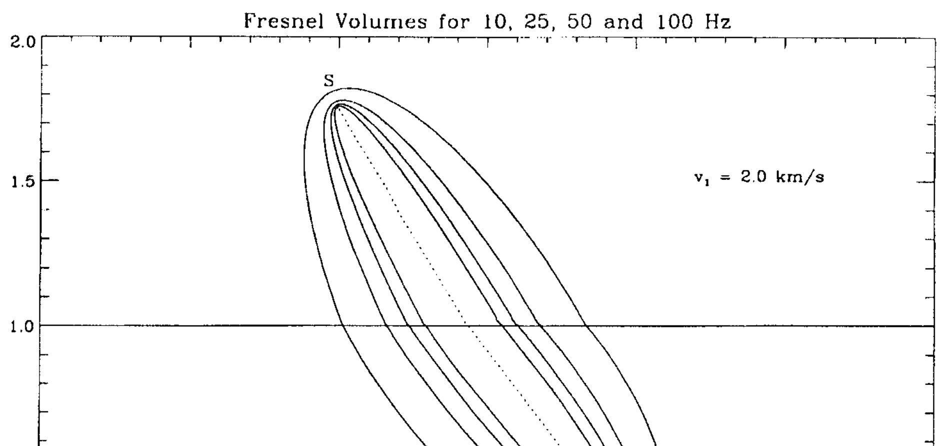

Fig. 5. Boundaries of the Fresnel volumes of transmitted waves for modest angles of incidence and four frequencies $f = 10$, 25, 50 and 100 Hz. The distances of source S and receiver R from interface Σ are the same, $h_R = h_S = 0{\cdot}75$ km. The offset (horizontal distance between S and R) equals 1 km. The velocity in the upper medium is 2 km/s, and in the lower medium 3 km/s.

The solution of (17) with (24) is as follows:

$$r^{\perp} = \sqrt{T}\left(\frac{1}{v_S \ell_S} + \frac{1}{v_R \ell_R}\right)^{-1/2} \quad . \tag{25}$$

It is interesting to note that (25) corresponds to (21) for $p = 0$.

One final remark. Equations (21), (22) and (23) assume that ray parameter $p = \sin i_S/v_S = \sin i_R/v_R$ of the transmitted wave SQR is known. If horizontal range r is known instead of p, ray parameter p must be determined from r using (19). For small p, we can determine it alternatively using the relation

$$p_{i+1} = r\left(\frac{h_S v_S}{\sqrt{1-v_S^2 p_i^2}} + \frac{h_R v_R}{\sqrt{1-v_R^2 p_i^2}}\right)^{-1} , \qquad i = 0,1,2, \ldots \quad , \tag{26}$$

starting with $p_0 = 0$. This yields $p_1 = r/\left(h_S v_S + h_R v_R\right)$, etc.

3.3 The interface Fresnel zone of transmitted waves for the angle of incidence close to the critical angle

If $v_R > v_S$ and the angle of incidence i_S is close to critical angle $i_S^* = \sin^{-1}\left(v_S/v_R\right)$, the form of the Fresnel volume of the transmitted wave will change drastically. See Fig. 6 as an example. This situation corresponds as a rule to the receiver being situated close to interface Σ beyond the critical point.

It is to some extent surprising that Eqs. (21) and (22) remain valid even in this case, if virtual point F is situated on the left-hand side of the point of incidence Q. We can prove this by considering the extreme case of receiver R situated directly on the surface beyond the critical point ($h_R = 0$). At distance L beyond the critical point, $\cos^2 i_S = 1 - n^2$, $\cos^2 i_R = 0$, and the first equation of (22) yields

$$\delta \approx \sqrt{\frac{T v_S \ell_S}{1-n^2}} \quad .$$

This corresponds fully to (7), derived for a similar situation for head waves in Section 2.1. This relation for δ is independent of L.

If horizontal range r is known instead of ray parameter p, ray parameter p must be determined from (19). In this case, however, iterative procedure (26) converges very slowly, as $\sqrt{1-v_R^2 p^2} = \cos i_R$ is very small. It is useful to introduce a new parameter, $Z = \sqrt{1-v_R^2 p^2}$, instead of p. We then obtain

$$p = \frac{\sqrt{1-Z^2}}{v_R} \quad , \qquad \sqrt{1-v_S^2 p^2} = \sqrt{1-n^2+n^2 Z^2} \quad . \tag{27}$$

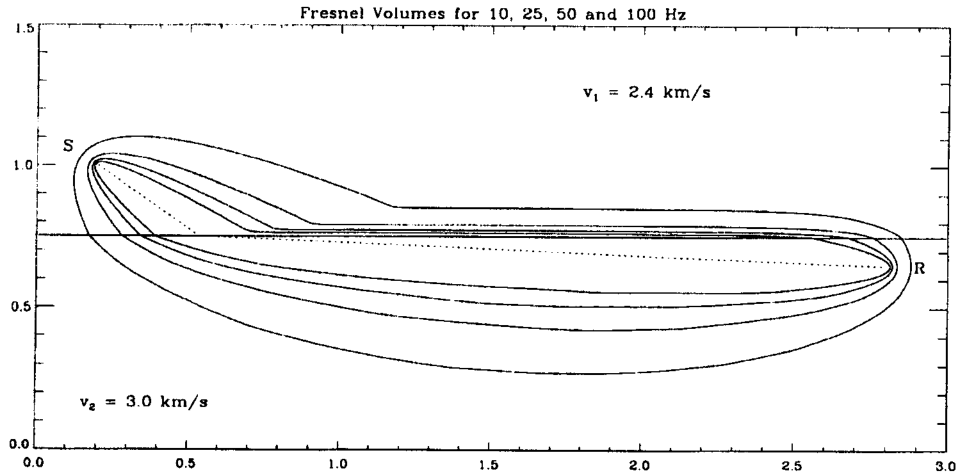

Fig. 6. The airplane shape of the boundary of the Fresnel volume of the transmitted wave, if the angle of incidence is close to the critical angle and if the distance of the receiver from interface Σ is small. The frequencies are 10, 25, 50 and 100 Hz, the distances of source S and receiver R from the interface are $h_S = 0{\cdot}25$ km and $h_R = 0{\cdot}1$ km, respectively. Note the penetration of the Fresnel volume across the interface back into the upper medium.

The iterative equation to determine Z is the as follows:

$$Z_{i+1} = h_R\sqrt{1-Z_i^2}\left(r - h_S n\sqrt{\frac{1-Z_i^2}{1-n^2+n^2Z_i^2}}\right)^{-1} , \quad i = 0,1,2,\ldots \quad , \tag{28}$$

starting from $Z_0 = 0$. The first approximation Z_1 for Z is then

$$Z_1 = \frac{h_R}{L} \quad , \qquad \text{where } L = r - \frac{h_S n}{\sqrt{1-n^2}} \quad . \tag{29}$$

Now we shall derive the dimensions of the interface Fresnel zone of the transmitted wave for virtual point F situated beyond critical point A, see Fig. 7. The ray of the transmitted wave is represented by trajectory SQR. Length δ is represented by $\overline{QA}$. It is not difficult to determine distance $q = \overline{FR'}$, where R' is the projection of R on Σ. It can be obtained from the equation

$$rp^* + \frac{h_S}{v_S}\sqrt{1-v_S^2 p^{*2}} + \frac{\sqrt{h_S^2+q^2}-q}{v_R} -$$
$$- rp - \frac{h_S}{v_S}\sqrt{1-v_S^2 p^2} - \frac{h_R}{v_R}\sqrt{1-v_R^2 p^2} = \frac{1}{2}T \quad ,$$

where $p^* = 1/v_R$, and p is determined from (19). If we replace p by Z, using (27), and apply (29), we obtain approximately for small Z,

$$\sqrt{h_R^2+q^2}-q=B \quad , \quad \text{where } B=\frac{1}{2}v_R T+\frac{1}{2}\frac{h_R^2}{L} \quad . \tag{30}$$

This finally yields

$$q \approx \frac{h_R^2-\left(\frac{1}{2}v_R T+\frac{1}{2}\frac{h_R^2}{L}\right)^2}{v_R T+\frac{h_R^2}{L}} \quad . \tag{31}$$

Note that q may be negative. In this case, point F is situated to the right of R'.

The *in-plane radius* $r^{\parallel}$ *of the interface Fresnel zone* becomes

$$r^{\parallel}=\frac{1}{2}(L+\delta-q) \quad , \tag{32}$$

where δ is given by (6) or (7), and q by (31). As we can see from (32), the in-plane radius $r^{\parallel}$ of the interface Fresnel zone of transmitted waves my be very large if the angle of incidence is nearly critical. It may even be larger than r, the horizontal range between S and R !

The *transverse semi-axis* of the interface Fresnel zone of the transmitted wave is again given roughly by equation (10), similarly as for head waves.

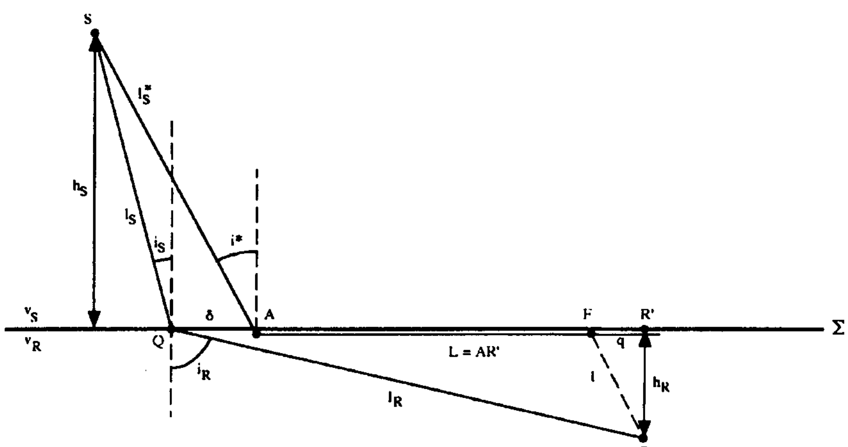

Fig. 7. Schematic diagram for the computation of distance q of virtual point F from projection R' of point R (receiver position) on the interface, $q=\overline{FR'}$. Point A is situated at the critical point on Σ, $L=\overline{AR'}$.

3.4 Penetration distances

Different types of penetrations can be studied for transmitted waves. For transmitted waves at small angles of incidence, the penetration distance on the bottom side of the interface has no sense, as the Fresnel volume does not terminate at the interface (as in the case of reflected waves), but continues regularly across it, see Fig. 5. The formulae for the transmitted waves are, however, applicable also to converted reflected waves, if the velocities are specified properly. In the case of converted reflected waves, the penetration over the interface has a very good physical meaning, and is similar to that of monotypic reflected wave.

Under near-normal incidence, the penetration distance of converted reflected waves, D, is again given by Eq. (32) of *Kvasnička and Červený (1996)*, where v_2 represents the compressional velocity below interface Σ. With increasing horizontal range between S and R, the penetration distance D increases slightly.

We shall now return to the monotypic transmitted waves. A very interesting picture can be observed for near-critical angles of incidence, see Fig. 6 and 8.

To investigate this situation analytically, we shall use the following notation. As in the case of head waves, we shall denote the penetration distance into the upper (lower-velocity) medium D^*. Approximately, D^* is given by the same equation (15) as for head waves.

The penetration distance D into the bottom medium is very complex due to non-vanishing distance h_R of receiver R from interface Σ. If distance h_R is zero or very small, penetration distance D is again given by (13), as for head waves. In case of transmitted waves, quantity L in (13), however, has the meaning $L = r - h_S n \big/ \sqrt{1-n^2}$. For non-vanishing h_R, we can relate penetration distance D to line AR (critical point - receiver), not to interface Σ. Equation (13) then remains approximately valid even for transmitted waves.

3.5 Numerical analysis

For *modest angles of incidence*, the interface Fresnel zones of transmitted waves have a similar character as those of reflected waves, see Fig. 5. The in-plane semi-axis $r^{\parallel}$ of the interface Fresnel zone of transmitted waves is given by relations (21), (22) or (23). Although the equations are only approximate, they provide excellent agreement with the values of $r^{\parallel}$ measured directly in Fig. 5.

If the *angles of incidence* are *close to the critical angle*, the character of Fresnel volumes of transmitted waves changes drastically. In this case, the Fresnel volumes have a typical airplane shape, see Figs. 6 and 8. They are considerably closer to head waves than to reflected waves. As in the case of head waves, the in-plane semi-axis $r^{\parallel}$ of the interface Fresnel zone of the transmitted wave is very long. As $r^{\parallel} = ½(L + \delta - q)$, see (32), in-plane semi-axis $r^{\parallel}$ can be calculated only after δ and q have been determined.

As we know from Section 2.1, the exact expressions for δ can be found for head waves, see (6). For transmitted waves, equations (20) or (21) derived for δ are not exact, but yield a very good approximation for the angle of incidence close to the critical angle (small h_R).

We shall now discuss the accuracy of Eq. (31) for q. By comparing the theoretical values obtained from (31) with those measured in Fig. 8, we find that the relative accuracy of Eq. (31) is rather low. In our examples, the accuracy is mostly close to 20–30%. Note that q can be close to zero or even negative. For example for $h_R = 0{\cdot}1$ km and $f = 10$ Hz, q

is negative, close to −0·03 km in Fig. 8. Equation (31) correctly yields q negative, but approximately equal to −0·04 km. However, small quantities such as −0·03 km are very difficult to measure in Fig. 8. In this case there may also be some inaccuracies in the network ray tracing computations. Moreover, the large relative errors in the small values of q do not affect the error in the computations of $r^{\parallel}$ very much.

We shall now compare the approximate theoretical values of $r^{\parallel}$ given by (32) with those measured in Figs. 6 and 8. We find that the accuracy of Eq. (32) is rather good. In most cases it is better than 5–7%. This is sufficiently accurate for most practical applications.

As proposed in Section 3.4, the equations for the penetration distances D^* and D, derived for head waves, can also be used for transmitted waves if the angle of incidence is close to the critical angle (small h_R). Equation (15) for the penetration distance D^* into the upper medium does not need any modifications at all, and its accuracy is very good. This can be checked in Figs. 6 and 8. The agreement is also good for the penetration distance D into lower medium, see (13). Here, however, we have to take into account two modifications. *First*, we have to use $L = r - h_S n / \sqrt{1-n^2}$, putting $h_R = 0$ in the expression for L corresponding to head waves. *Second*, we have to measure D from the geometrical ray (see the dotted line in Fig. 8), not from the interface. If we measure D from the geometrical ray, accuracy is good, better than 10%. The penetration distance D, measured from the geometrical ray, can be simply reduced to the penetration distance measured from Σ using simple geometrical considerations.

4. CONCLUDING REMARKS

As in Part 1 of this paper, we shall discuss the applicability of Fresnel volume ray tracing (based on paraxial ray approximation, see *Červený and Soares*, 1992) to head and transmitted waves.

Let us first consider the Fresnel volumes of transmitted waves for modest angles of incidence, see Section 3.2. The transmitted waves are in this case quite regular, zero-order waves in the terminology of the ray method. Fresnel volume ray tracing is fully applicable to such waves, and will yield results corresponding to (21)–(23).

For the transmitted waves with angles close to the critical angle, it would be, in principle, also possible to use the paraxial ray approximation, but the accuracy of the computations will be lower. There are two reasons for it. *First*, the paraxial ray approximation is based on dynamic ray tracing and this yields results of lower accuracy for near-critical computations. *Second*, interface Σ is situated very close to the segment of the ray of the transmitted wave between points Q (reflection/transmission point) and R (receiver). The method of paraxial ray approximation cannot take into account the proximity of Σ to the ray, as it is fully based on the local medium parameters and their derivatives along the ray. Thus, Fresnel volume ray tracing will not yield sufficiently accurate results in regions where the ray roughly copies interface Σ. It cannot, of course, provide any information on the penetration across Σ into the upper medium and on penetration distance D^*.

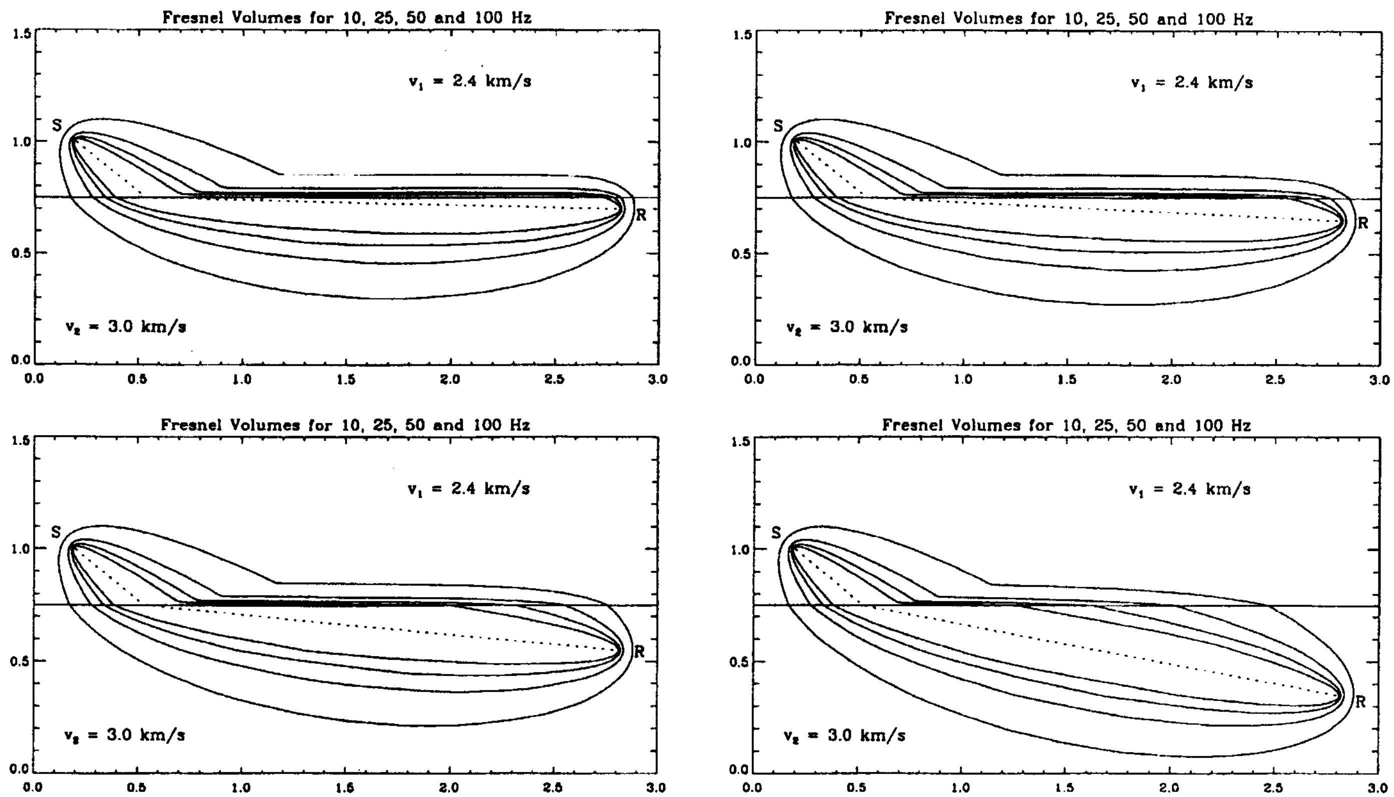

Fig. 8. Boundaries of the Fresnel volumes of transmitted waves if the angle of incidence is close to the critical angle, and for various distances h_R of receiver R from interface Σ, $h_R = 0{\cdot}05, 0{\cdot}1, 0{\cdot}2$ and $0{\cdot}4$ km The frequencies are 10, 25, 50 and 100 Hz, distance h_S of source S from interface Σ is $h_S = 0{\cdot}25$ km. The velocity in the upper medium is again 2·4 km/s and in the lower medium 3 km/s, so that the index of refraction $n = 0{\cdot}8$.

Note that Fresnel volume ray tracing will usually provide a good estimate of the Fresnel volumes of transmitted waves along segment $\overline{QR}$ even if the angle of incidence is close to the critical angle, but only on the side of the geometrical ray opposite to Σ. Consequently, Fresnel volume ray tracing will yield a fairly accurate value of D.

An additional remark on the transmitted waves. We have only investigated the case of $v_R > v_S$. The case of $v_R < v_S$ may, of course, also be considered. All the above results my again be applied, only source S and receiver R have to be replaced. The complications related to the critical angle will appear for angles of incidence close to ½π and if h_S is small. The angle of transmission will be close to the critical angle in this case. All the figures presented here apply, they have only to be viewed upside down.

As the concept of Fresnel volumes is fully based on kinematical quantities (travel times), we can use the same concept also for reflected and transmitted converted waves. All the equations presented in this paper remain valid, only velocities v_S and v_R have to be specified properly. The penetration of the Fresnel volume across interface Σ can also be studied for reflected converted waves. See the discussion in Section 3.4. This penetration cannot, of course, be obtained by Fresnel volume ray tracing, see *Červený and Soares (1992)*.

The case of head waves is considerably more complex. The head wave is not a wave of the zero-order ray approximation of the ray theory, but a wave of the first-order approximation. The standard Fresnel volume ray tracing, based on the paraxial ray approximation, cannot be applied to such waves.

Acknowledgements: This work was partially supported by the Elf Geoscience Research Centre, London, U.K., by the Grant Agency of the Charles University under Contract 8/94 [and 38/94], by the Grant Agency of the Czech Republic under Contract 205/95/1465, and by the European Commission within the framework of the JOULE II Project "Integrated Structural Imaging of Seismic Data".

Manuscript received: 18 January 1995; Revised: 20 December 1995

References

Červený V. and Soares J.E.P., 1992: Fresnel volume ray tracing. *Geophysics* **57**, 902–915.

Eaton D.W.S., Stewart R.R. and Harrison M.P., 1991: The Fresnel zone for P-SV waves. *Geophysics* **56**, 360–364.

Hubral P., Schleicher J., Tygel M. and Hanitzsch C., 1993: Determination of Fresnel zones from traveltime measurements. *Geophysics* **58**, 703–712.

Kvasnička M. and Červený V., 1994: Fresnel volumes and Fresnel zones in complex laterally varying structures. *J. Seismic Exploration* **3**, 215–230.

Kvasnička M. and Červený V., 1996. Analytical expression of Fresnel volumes and interface Fresnel zones of seismic body waves. Part 1: Direct and unconverted reflected waves. *Studia geophys. geod.* **40**, 136–155.